NANO LETTERS

2007
Vol. 7, No. 3
626−631

Photoluminescence of GaN Nanowires of Different Crystallographic Orientations

Alan H. Chin,*,† Tai S. Ahn,‡ Hongwei Li,§,|| Sreeram Vaddiraju,§,⊥ Christopher J. Bardeen,‡ Cun-Zheng Ning,*,† and Mahendra K. Sunkara§

Center for Advanced Aerospace Materials and Devices, NASA Ames Research Center, Moffett Field, California 94035; Department of Chemistry, University of California, Riverside, California 92521; and Department of Chemical Engineering, University of Louisville, Louisville, Kentucky 40292

Received October 26, 2006; Revised Manuscript Received January 24, 2007

ABSTRACT

We utilized time-integrated and time-resolved photoluminescence of *a*-axis and *c*-axis gallium nitride nanowires to elucidate the origin of the blue-shifted ultraviolet photoluminescence in *a*-axis GaN nanowires relative to *c*-axis GaN nanowires. We attribute this blue-shifted ultraviolet photoluminescence to emission from surface trap states as opposed to previously proposed causes such as strain effects or built-in polarization. These results demonstrate the importance of accounting for surface effects when considering ultraviolet optoelectronic devices based on GaN nanowires.

GaN nanowires have been the subject of intense research lately due to the many potential applications (lasers, light-emitting diodes, modulators, detectors, etc.)[1−3] and interesting properties[4,5] that they possess. Because GaN has a wurtzite crystal structure, which is an anisotropic crystal structure, many of its properties are dependent upon crystal orientation. For example, the photoluminescence (PL) of GaN nanowires in the ultraviolet (UV) has been observed to depend on the growth direction of GaN.[4,5] However, the origin of the difference in PL between nanowire samples of different growth directions remains unclear. Understanding the cause of this difference can have significant impact on improving the performance of future optoelectronic devices based on GaN nanowires, as the nature of the different PL sources (e.g., band edge, defects, etc.) can impact device performance (e.g., gain).[6] Previous attempts to explain the dependence of PL on GaN growth direction have invoked various phenomena: strain in the nanowires,[7] dopants,[8] or built-in polarization.[5] The spontaneous built-in polarization, which is responsible for the PL peak shift in quantum wells,[9] can be ruled out. In quantum well growth, the growth perpendicular to the (001) polar surface (*c*-plane) will result in a built-in field, which leads to red-shift of the PL peak. In the case of nanowires, because the field along wire direction can be ignored due to the relatively large distance (∼10 μm), growth along the ⟨001⟩ direction (along the *c*-axis) will not result in a significant built-in field. Rather, growth along the ⟨1−10⟩ direction (along the *a*-axis) could result in a large built-in potential, but the blue-shift of PL in the *a*-axis nanowire is not consistent with such an explanation. Given that the surface plays such an important role in nanoparticles (due to the high surface-to-volume ratio) and the majority of the luminescent material is in proximity to the surface (half of the volume of a 20 nm diameter nanowire is within ∼3 nm of the surface), perhaps the nature of the surfaces (termination, shape, strain, defects, etc.) can account for the difference, as has been suggested by other studies.[10−13] In the extreme case of spherical nanoparticles, it is now well-established that oxide surface-state luminescence can significantly contribute to the PL.[12,13] To determine if surface states play a role in the dependence of GaN nanowire photoluminescence on crystal orientation, we use time-integrated photoluminescence (TIPL) and time-resolved photoluminescence (TRPL) to study the PL from GaN nanowire samples of different crystallographic orientation.

We utilized two different UV PL setups to study the TIPL of GaN nanowires. One setup was a commercial Raman

* Corresponding authors. E-mail: achin@mail.arc.nasa.gov (A.H.C.); cning@mail.arc.nasa.gov (C.-Z.N.).
† Center for Advanced Aerospace Materials and Devices, NASA Ames Research Center.
‡ Department of Chemistry, University of California.
§ Department of Chemical Engineering, University of Louisville.
|| Current address: Department of Materials Science and Engineering, Lehigh University, Bethlehem, Pennsylvania 18015.
⊥ Current address: Department of Chemical Engineering, Massachusetts Institute of Technology, Cambridge, Massachusetts 02139.

10.1021/nl062524o CCC: $37.00
Published on Web 02/27/2007

scattering and PL system (Renishaw inVia Raman microscope) that uses a 325 nm continuous-wave (CW) He−Cd UV laser as an excitation source. The PL was collected by an objective lens, directed to a spectrometer, and detected by a thermoelectrically cooled CCD detector. While a laser-heating-induced red-shift was observed at the highest excitation intensities with this setup, the data shown here are with low excitation intensity to avoid laser-heating effects. The other setup was based on a passively mode-locked Ti:sapphire laser (810 nm, ∼150 fs pulse duration, 80 MHz repetition rate, 1.5 W average power) that was frequency tripled to yield ∼100 mW average power of light at 271 nm. This pulsed (∼200 fs pulse duration) UV beam was focused by a 500 mm focal length lens and directed to the sample at ∼70° from normal, yielding a spot size of ∼60 μm × 180 μm. This led to a maximum *average* intensity of ∼900 W/cm^2 and a maximum *peak* intensity of ∼6 × 10^7 W/cm^2 per pulse on the sample. The PL was collected by a UV objective (13×), directed into a 0.3 m spectrometer, and detected with a liquid-nitrogen-cooled CCD detector. The spectral resolution of this system can be as high as ∼0.2 nm. For TRPL, we used ultrashort pulses at 267 nm obtained from the frequency-tripled output of a 40 kHz regeneratively amplified Ti:sapphire laser system with a 150 fs pulse width. The maximum *average* laser intensity on the sample is less than 400 W/cm^2. The PL of the samples was collected at 45° relative to the excitation beam. The PL is collimated and focused into a spectrometer to disperse the spectrum before being passed to a picosecond streak camera (Hamamatsu C4334 Streakscope). The instrument response is ∼15 ps in a 1 ns sweep window, and the spectral resolution is 2 nm.

We studied GaN nanowires of comparable diameters with growth directions ⟨001⟩, along the *c*-axis, and ⟨1−10⟩, along the *a*-axis. Growth of these nanowires has been described elsewhere.[4] Briefly, direct nitridation of Ga melts on a substrate in the presence of ammonia or a mixture of nitrogen and hydrogen plasma forms *c*-axis GaN nanowires, and vapor transport of Ga in the presence of dissociated ammonia forms *a*-axis GaN nanowires on a previously bare substrate. Note that the *a*-axis GaN nanowires studied here have both Ga- and N-terminated {001} surfaces and a rectangular cross-section, as opposed to only one {001} surface and a triangular cross-section in the case of the work of the Yang group.[5] The GaN nanowires formed by either method are studied as-synthesized on the growth substrates. The average diameter distribution of the nanowires is peaked at ∼20 nm for samples of both growth directions. The substrates used are either amorphous quartz glass or graphite.

To gain insight into the PL mechanisms for the two types of GaN nanowire samples, we first examined the TIPL of the two types of samples with the substrates at room temperature. Figure 1 shows PL from *c*-axis GaN nanowires on glass and *a*-axis GaN nanowires on graphite. There is a significant difference of the PL peak position for the *a*-axis GaN nanowires compared to the *c*-axis GaN nanowires. This ∼140 meV blue-shift (the difference in the centroids of the PL data from the two types of nanowires is ∼100 meV) is

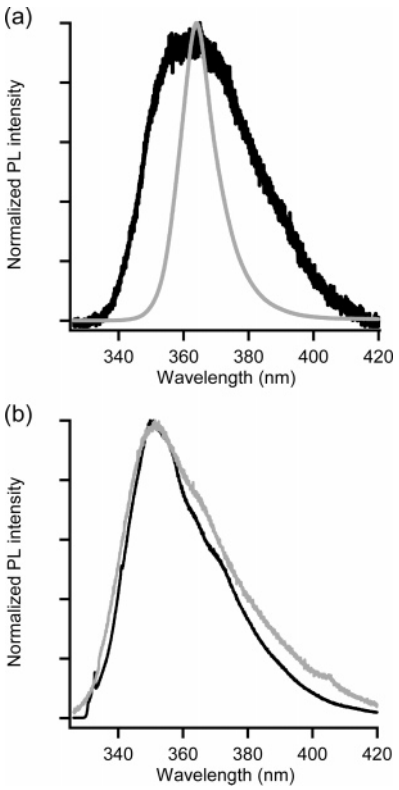

Figure 1. Comparison of *c*-axis and *a*-axis GaN nanowire photoluminescence: (a) *c*-axis GaN nanowires (black) and polycrystalline GaN (gray) at low CW power; (b) *a*-axis GaN nanowires using pulsed laser excitation (gray) and low CW power laser excitation (black).

comparable to a previous observation of crystal orientation-dependent PL in GaN nanowires.[5] In addition, as seen in Figure 1a, the PL peak position for the *c*-axis GaN nanowires is close to the expected value for bulk GaN at room temperature (3.4 eV, or 365 nm) and is broader but centered at the PL peak position of polycrystalline GaN. The PL peak broadening may be due to point-defect incorporation in the nanowires or a distribution of strain/stress in the nanowires that affects the excitonic emission (e.g., by affecting the donor-bound exciton emission). In Figure 1b, the PL data for the *a*-axis GaN nanowires from the CW PL setup compares well with the pulsed PL setup, indicating that there is no significant peak intensity effect on the PL. Note that the peak positions for both types of GaN nanowires are significantly higher in photon energy than in previous observations.[5,7] This difference may be caused by a difference in strain between our nanowires and those of the other groups. This difference may also be caused by red-shifting of the PL emission due to heating by the excitation laser used by the other groups, as it has been shown that significant sample heating can occur in nanowires[4] and nanoparticles[14] with high CW (or average, for pulsed lasers) laser intensity (∼10 kW/cm^2). The data shown here is taken with <1 kW/cm^2, where no significant red-shift from laser heating is observed. In addition to the blue-shift, this data also indicates asymmetry in the PL peak for *a*-axis GaN nanowires. This asymmetry seems to suggest a contribution to the PL of an additional species that has PL emission at ∼350 nm (3.54

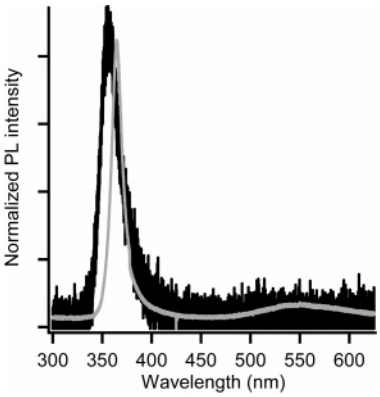

Figure 2. Comparison of photoluminescence from *a*-axis GaN nanowires (black) and polycrystalline GaN (gray) using pulsed laser excitation. Note that a KG3 colored glass filter with a 50% cutoff at ~330 nm is used, which slightly modifies the line shape to the blue of 350 nm.

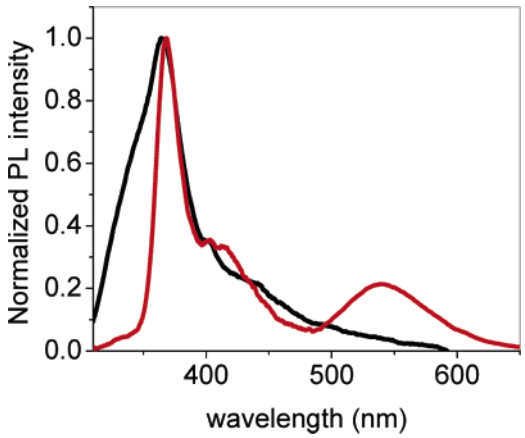

Figure 3. Photoluminescence spectrum of the streak camera data integrated over all times for *a*-axis GaN nanowires (black) and polycrystalline GaN (red).

eV) that is blue-shifted relative to the GaN band-edge PL at 365 nm (3.4 eV).

To further study this blue-shifted feature, we examined a similar *a*-axis GaN nanowire sample (this time, on a glass substrate) to the sample used for the data in Figure 1. Figure 2 shows the TIPL (using the Ti:sapphire-based TIPL setup) from a spot on the *a*-axis GaN nanowire sample with dense nanowire coverage and from a polycrystalline GaN sample. Note that there is a colored glass filter used that attenuates the PL for wavelengths shorter than ~330 nm. Again, as in Figure 1, there is a significant blue-shift and broadening of the *a*-axis GaN nanowire PL compared to the polycrystalline GaN PL peak in the UV. Figure 3 shows the corresponding TIPL from the TRPL setup, which shows similar TIPL response for *a*-axis GaN nanowires (black curve). Because the sample was not optimized for homogeneous growth over relatively large distances (on the order of 1 mm) on the substrate, the nanowire density varies over the substrate. As a result, there are regions that do not exhibit the blue-shifted feature, where there is lower nanowire coverage, but retain a luminescence contribution from a GaN thin film with nonuniform morphology. These regions have a UV peak that matches the polycrystalline GaN, but are different in visible PL. This difference in visible PL is likely due to the morphology of the GaN film, as has been observed in ZnO nanostructures.[15] Because of the relatively large (~100 μm) excitation spot size for the TRPL setup, the data has some contribution from regions of low nanowire coverage, which accounts for some of the difference between the data in Figures 2 and 3. In addition, there is no filtering of light to the blue of 350 nm, which makes the blue-shifted feature more pronounced to the blue in the data in Figure 3 compared to the data in Figure 2. On the basis of this TIPL data, we assign any blue-shifted PL from 310 to 350 nm to be from the *a*-axis GaN nanowires.

The TRPL behavior of the *a*-axis GaN nanowires relative to polycrystalline GaN provides further information about this blue-shifted feature. Figure 4a shows the normalized temporal response of the two samples in the spectral window from 350 to 390 nm, which is around the UV PL peak of bulk GaN, i.e., the polycrystalline GaN UV PL peak. Two main features are present in this data. First, both the *a*-axis GaN nanowire sample and the polycrystalline GaN sample show very rapid initial luminescence decays in this spectral window. Second, the *a*-axis GaN nanowire sample has an additional longer-lived component. Figure 4b shows normalized TRPL data from the spectral window from 310 to 350 nm, where the decay time of the now-dominant long-lived component is 0.50 ns, very similar to the 0.45 ns decay time of the long-lived component in the 350−390 nm spectral window. In the 310−350 nm spectral window, the nanowire decay reflects predominantly the longer-lived component. The emission intensity from the nanowires in this wavelength range is significantly *higher* than that from the polycrystalline GaN, which has data of insufficient signal-to-noise ratio from which to extract a useful decay time. The data from Figure 4a and b suggest that there is a long-lived spectral feature in the nanowires that is broader than the bulk GaN UV feature, extending from at least 310 to 390 nm. Note that changing the excitation laser intensity by a factor of 2 does not change the spectra or the dynamics, ruling out any intensity-dependent effects.

To determine the spectral shape of the blue-shifted feature, we examined time-resolved spectra integrated over different temporal windows of the TRPL data. Figure 5a shows the normalized PL spectra from the nanowire sample, integrated over three temporal ranges: 0−100 ps, 500−600 ps, and 1−5 ns after laser excitation. The 0−100 ps data show that the early time response is dominated by the bulk GaN UV PL, whose emission is almost completely quenched after ~100 ps, as seen in the data in Figure 4. The 1−5 ns data show the longer-lived spectral features. In particular, the blue-shifted spectral feature is shown to indeed cover the spectral range from 310 to 390 nm. In addition, there is a spectral feature around 440 nm and a tail out to ~600 nm. These features in the visible spectral range may be a combination of the longer-lived spectral features at ~430 and ~520 nm observed in the polycrystalline GaN spectra in Figure 5b. The 550 nm peak is the yellow emission that is often observed in bulk GaN.[16]

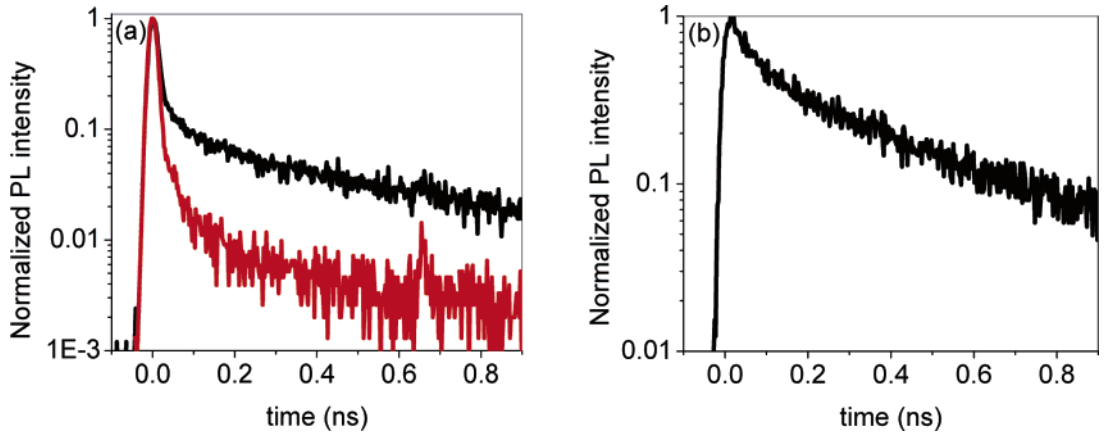

Figure 4. Time decay of the photoluminescence signal in the spectral window of (a) 350−390 nm for the *a*-axis GaN nanowires (black) and polycrystalline GaN (red); (b) *a*-axis GaN nanowire decay in the 310−350 nm spectral window. The photoluminescence signal of polycrystalline GaN in the latter window has insufficient signal-to-noise ratio to extract a useful decay time.

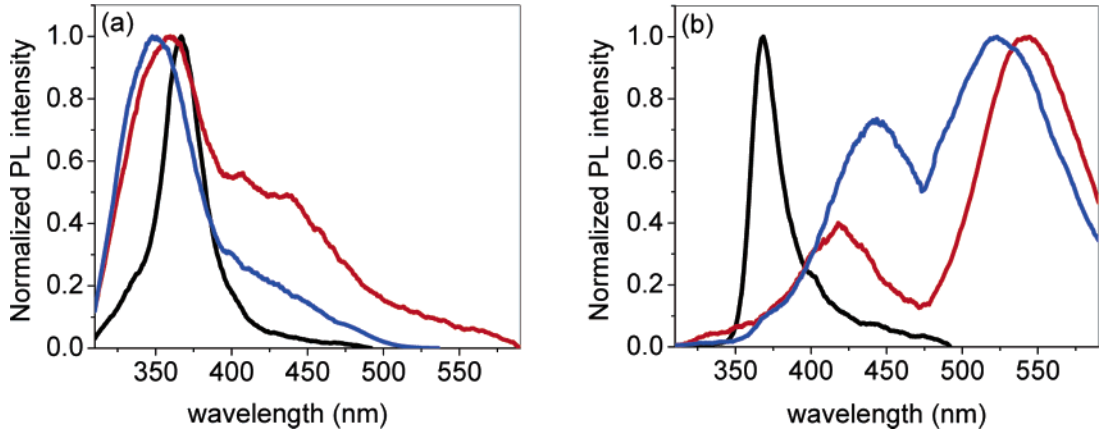

Figure 5. Photoluminescence spectra of (a) *a*-axis GaN nanowires and (b) polycrystalline GaN at 0−100 ps (black), 500−600 ps (blue), and 1−5 ns (red) after laser excitation.

More information about the nature of the blue-shifted spectral feature can be obtained by concentrating on the early temporal response of this feature relative to the bulk GaN UV response. In Figure 6, we compare the early temporal response of the nanowires in the spectral window from 310 to 350 nm, where primarily only the blue-shifted PL exists, to the spectral window from 350 to 390 nm, where primarily only bulk GaN PL exists. The instrument response is also shown in the figure. Although the dynamics are close to the instrument resolution of the streak camera, we can simultaneously fit both the decay of the bulk emission along with the growth of the blue-shifted emission with a single time constant $\tau = 5$ ps. It should be emphasized that this value is approximate due to our limited time resolution and that the actual value of τ probably lies within the range of 3−10 ps. The main point is that the wavelength-dependent dynamics in the 300−400 nm spectral window can be explained by a single process where a fraction of the short-lived bulk electron−hole pairs (initially formed with significant excess energy due to the large pump laser photon energy) are prevented from relaxing to the conduction and valence band edges and emitting around 365 nm, but are instead transformed into long-lived species that emit around 350 nm. This transformation occurs on a time scale of 10 ps or less. This

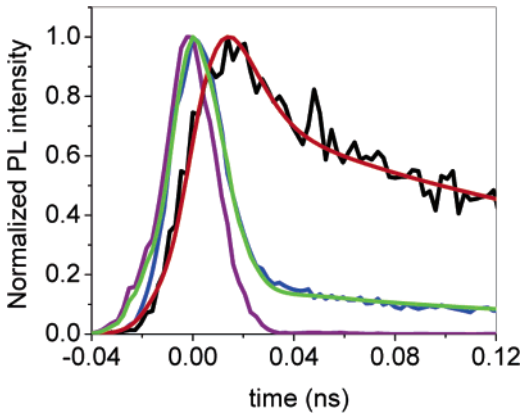

Figure 6. Time evolution of the photoluminescence signal for *a*-axis GaN nanowires in the spectral window of 310−350 nm (black), in the spectral window of 350−390 nm (blue), and their convoluted fits (red and green, respectively) using the temporal resolution of the instrument obtained by measuring the scattered light at 266 nm (purple). The initial decay time of the green line and the initial rise time of the red line were both 5 ps.

is suggestive of a surface trapping process occurring, where some fraction of electron−hole pairs are prevented from recombining via the bulk emission process because carriers diffuse to the surface where they are trapped before carrier

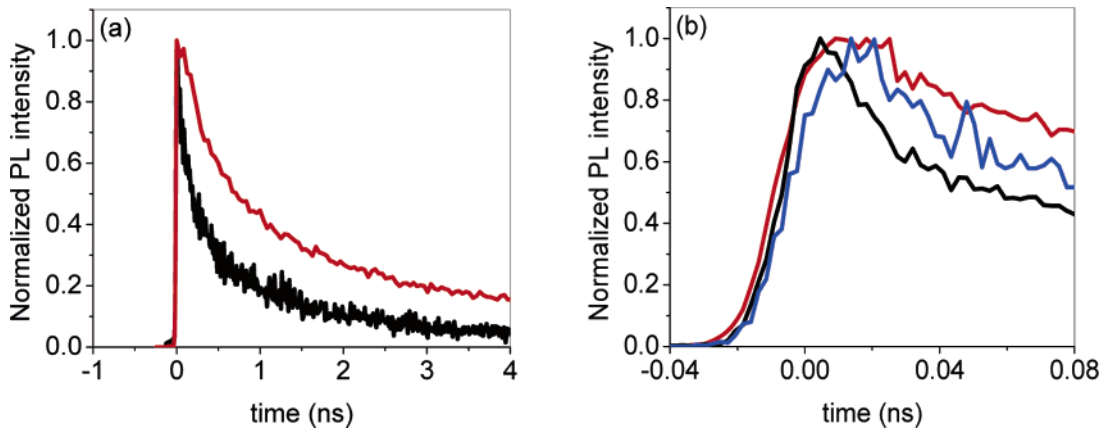

Figure 7. (a) Time decay of the photoluminescence signal for *a*-axis GaN nanowires in the spectral window of 410−590 nm (black) and polycrystalline GaN in spectral window of 480−660 nm (red). (b) Same as (a), with the decay for the nanowires in the spectral window of 310−350 nm (blue) superimposed.

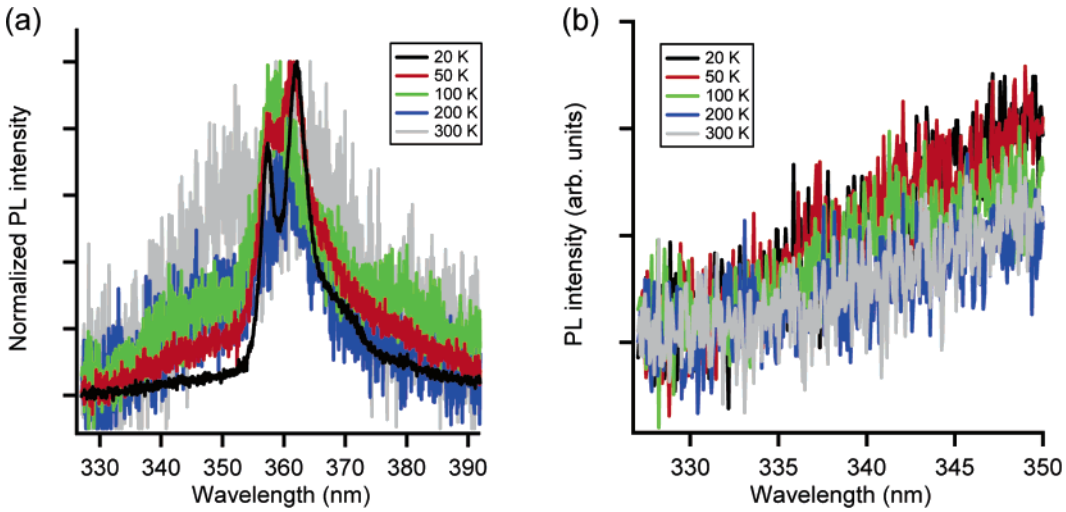

Figure 8. Low-temperature photoluminescence of *a*-axis GaN nanowires: (a) normalized photoluminescence data; (b) photoluminescence data in the spectral region from 325 to 340 nm, demonstrating relatively small temperature dependence of the photoluminescence in this region. Note that a KG3 colored glass filter with a 50% cutoff at ~330 nm is used, which slightly modifies the line shape to the blue of 350 nm.

relaxation to the band edge is complete. Once a carrier is trapped and localized at a surface trap state, light emission primarily occurs when the complementary carrier diffuses to the same surface trap. To estimate a diffusion velocity for carrier trapping, if we assume that carriers can traverse a 20 nm diameter nanowire in the trapping time of ~10 ps, we get a carrier diffusion velocity of $\sim 2 \times 10^7$ cm/s. This is a reasonable carrier diffusion velocity, as electron drift velocities in GaN are of this order of magnitude.[17]

One question to ask is whether the other longer-lived emission species observed in the nanowires are related to surface trapping. To answer this question, in Figure 7a, we examined the temporal response of the red-shifted longer-lived species shown in Figure 5. We see that the nanosecond decays for both the nanowires and the polycrystalline GaN are comparable, which indicates that the emission is not related to the bulk band edge emission. Moreover, in Figure 7b, in both samples, it appears the longer-wavelength emission does not have a resolvable rise-time nor does it have an appreciable decay component on the 10 ps time scale. The 480−660 nm emission in polycrystalline GaN is attributed to Ga vacancies,[16] which may be randomly distributed throughout the sample. Because there will be carriers that do not need to diffuse to become trapped by these vacancies and emission from them can decay independently of the bulk GaN emission, this type of emission would be expected to have an instantaneous rise and a sample-independent decay. The similarity of the two decays in Figure 7a suggests that the 410−590 nm emission from the *a*-axis GaN nanowire sample may have a similar origin. As shown in Figure 7b, only the response from the blue-shifted PL feature seems to show a resolvable rise time, indicating that this is the only PL feature that is related to diffusion to the surface.

Finally, to gain additional insight into the source of the blue-shifted PL from *a*-axis GaN nanowires, we studied the temperature-dependent PL (using the Ti:sapphire-based TIPL system) behavior of the GaN nanowires, where the substrate temperature is lowered to cryogenic temperatures in a microscope-compatible cryostat. Figure 8a shows the nor-

malized temperature-dependent PL from *a*-axis GaN nanowires on graphite. Note that for this area of the sample, there is some PL contribution from an underlying thin film of GaN that covers the substrate. Figure 8b shows the temperature-dependent PL in the spectral range where the blue-shifted spectral feature is dominant. The main features of the data are: (1) insignificant shifting of the blue-shifted PL peak with temperature, (2) relatively small increase of the blue-shifted PL peak with lower temperature, and (3) significant enhancement of the bulk GaN PL at lower temperatures (the PL signal at 362 nm at 20 K is 28 times the PL signal at 300 K). The broad, relatively temperature-insensitive blue-shifted PL emission from the *a*-axis GaN nanowires is similar to defect emission in ZnO nanostructures.[15] This data provides further evidence that the blue-shifted emission from *a*-axis GaN nanowires is not due to bulk GaN emission, which is consistent with the surface-state emission picture presented above.

The nature of the surface trap states that may cause this blue-shifted emission is related to the nature of the *a*-axis GaN nanowire surfaces relative to the *c*-axis GaN nanowire surfaces, as a pronounced blue-shifted feature is not observed for *c*-axis GaN nanowire samples. Blue-shifting of the bulk band gap due to surface strain[18] can be ruled out because it is not observed in *c*-axis GaN nanowire samples and because the temporal response and temperature-dependent response is much different than the bulk GaN PL response. We speculate that a thin oxide layer forming at the surface introduces surface traps that cause the blue emission and that the *a*-axis GaN nanowire surfaces are more susceptible to oxidation than the *c*-axis GaN nanowire surfaces. Ga_2O_3 has been shown to exhibit emission in the spectral range of the blue-shifted PL.[19] Because there is more Ga-terminated *c*-axis surface for the *a*-axis GaN nanowires, perhaps oxidation of this surface leads to the formation of surface trap states. Oxidation of GaN is very difficult due to the stability of GaN, but oxidation is more likely to occur at N-terminated surfaces with N vacancies or Ga-terminated surfaces,[20] so we speculate that the Ga- and N-terminated {001} surfaces of the *a*-axis GaN nanowires are more susceptible to oxidation. Different defects at the surfaces of the *a*-axis GaN nanowires relative to the *c*-axis GaN nanowires may also be the cause of the blue-shifted feature. Defects not at the surface can be ruled out because they should exhibit instantaneous temporal response. Further study is needed to confirm the true nature of the surface trap states such as studies with nanowires of different diameter or of different surface treatment.

In conclusion, we have observed crystal-orientation-dependent PL in GaN nanowires. We attribute the blue-shifted PL of *a*-axis GaN nanowires to surface states that act as traps of photoexcited carriers. These results demonstrate the importance of surface states to the PL of GaN nanowires and the importance of controlled nanowire growth orientation on the optical properties of GaN nanowires. Our results are relevant for GaN nanowire optoelectronic devices, as eliminating such surface-state emission can improve the performance of lasers or light-emitting diodes based on GaN nanowires by improving the efficiency of the pathway toward the more efficient band edge emission.

Acknowledgment. We thank Chandrashekhar Pendyala for his assistance with GaN nanowire fabrication and characterization. A.H.C. is employed by ELORET Corporation, and his work at NASA Ames Research Center (ARC) is supported by a subcontract from the University Affiliated Research Center (UARC), operated by the University of California, Santa Cruz. C.Z.N. is with UARC. The work of S.V. at NASA ARC is supported by NASA-JRI-NNA05CS49A. H.L., S.V., and M.K.S. acknowledge support from the Kentucky Science and Engineering Foundation (KSEF-148-502-04-86) and the U.S. DOE (DE-FG0205ER64071) for supporting the Institute for Advanced Materials at the University of Louisville. C.J.B. acknowledges the support of the National Science Foundation (CHE-0517095).

References

(1) Greytak, A. B.; Barrelet, C. J.; Li, Y.; Lieber, C. M. *Appl. Phys. Lett.* **2005**, *87*, 151103.
(2) Zhong, Z. H.; Qian, F.; Wang, D. L.; Lieber, C. M. *Nano Lett.* **2003**, *3*, 343−346.
(3) Sirbuly, D. J.; Law, M.; Yan, H. Q.; Yang, P. D. *J. Phys. Chem. B* **2005**, *109*, 15190−15213.
(4) Li, H.; Chin, A. H.; Sunkara, M. K. *Adv. Mater.* **2006**, *18*, 216−220.
(5) Kuykendall, T.; Pauzauskie, P. J.; Zhang, Y. F.; Goldberger, J.; Sirbuly, D.; Denlinger, J.; Yang, P. D. *Nat. Mater.* **2004**, *3*, 524−528.
(6) Gradečak, S.; Qian, F.; Li, Y.; Park, H.-G.; Lieber, C. M. *Appl. Phys. Lett.* **2005**, *87*, 173111.
(7) Seo, H. W.; Bae, S. Y.; Park, J.; Yang, H. N.; Park, K. S.; Kim, S. *J. Chem. Phys.* **2002**, *116*, 9492−9499.
(8) Xu, C.; Chung, S.; Kim, M.; Kim, D. E.; Chon, B.; Hong, S.; Joo, T. *J. Nanosci. Nanotechnol.* **2005**, *5*, 530−535.
(9) Waltereit, P.; Brandt, O.; Trampert, A.; Grahn, H. T.; Menniger, J.; Ramsteiner, M.; Reiche, M.; Ploog, K. H. *Nature* **2000**, *406*, 865−868.
(10) Chen, C.-W.; Chen, K.-H.; Shen, C.-H.; Ganguly, A.; Chen, L.-C.; Wu, J.-J.; Wen, H.-I.; Pong, W.-F. *Appl. Phys. Lett.* **2006**, *88*, 241905.
(11) Shalish, I.; Temkin, H.; Narayanamurti, V. *Phys. Rev. B* **2004**, *69*, 245401.
(12) Biteen, J. S.; Lewis, N. S.; Atwater, H. A.; Polman, A. *Appl. Phys. Lett.* **2004**, *84*, 5389−5391.
(13) Niquet, Y. M.; Allan, G.; Delerue, C.; Lannoo, M. *Appl. Phys. Lett.* **2000**, *77*, 1182−1184.
(14) Bergman, L.; Chen, X. B.; Morrison, J. L.; Huso, J.; Purdy, A. P. *J. Appl. Phys.* **2004**, *96*, 675−682.
(15) Djurisic, A. B.; Leung, Y. H.; Tam, K. H.; Ding, L.; Ge, W. K.; Chen, H. Y.; Gwo, S. *Appl. Phys. Lett.* **2006**, *88*, 103107.
(16) Nam, K. B.; Nakarmi, M. L.; Lin, J. Y.; Jiang, H. X. *Appl. Phys. Lett.* **2005**, *86*, 222108.
(17) Jain, S. C.; Willander, M.; Narayan, J.; Van Overstraeten, R. *J. Appl. Phys.* **2000**, *87*, 965−1006.
(18) Pozina, G.; Edwards, N. V.; Bergman, J. P.; Paskova, T.; Monemar, B.; Bremser, M. D.; Davis, R. F. *Appl. Phys. Lett.* **2001**, *78*, 1062−1064.
(19) Zhang, J.; Jiang, F. H. *Chem. Phys.* **2003**, *289*, 243−249.
(20) Watkins, N. J.; Wicks, G. W.; Gao, Y. L. *Appl. Phys. Lett.* **1999**, *75*, 2602−2604.

NL062524O